Electronic Supplementary Material (ESI) for ChemComm.


**Supporting Information**

# Fused tetraphenylethylene-triphenylamine for efficient hole transporting materials in perovskite solar cells

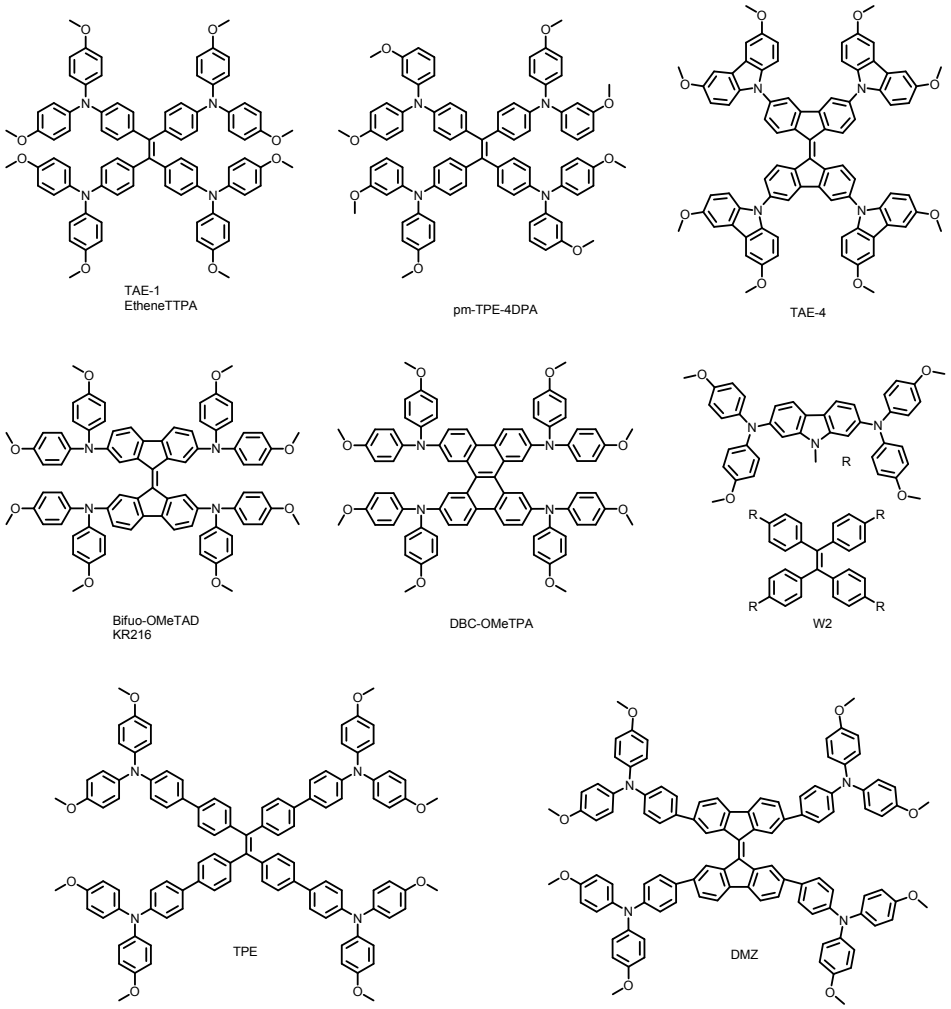


**Scheme S1** The molecular structures of reported tetraphenylethylene-based HTM.

## Experimental Section

### Materials

All reagents and chemicals are purchased from Sigma-Aldrich, TCI, Alfa or Sinopharm Chemical Reagent Co., et al. THF is dried by 4A molecular sieves under dark for several days. Other chemicals are used as received without further processing unless otherwise noted. The reference non-fused tetraphenylethylene-based compound (**TPE**) is prepared *via* Suzuki-Miyaura and McMurry cross-coupling reactions in our lab referring to previous literature.[1]

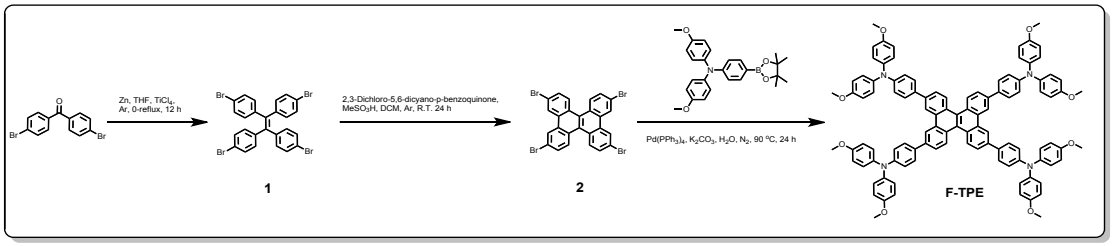


**Scheme S2** Synthetic route to fused tetraphenylethylene-triphenylamine molecule.

**Synthesis of investigated molecules**

The key intermediate, 4-methoxy-N-(4-methoxyphenyl)-N-(4-(4,4,5,5-tetramethyl-1,3,2-dioxaborolan-2-yl)phenyl)aniline, is sequentially prepared in our lab through Ullmann and Miyaura-Ishiyama-Hartwig Borylation reactions according to the literature. The target fused tetraphenylethylene-triphenylamine product is sequential synthesized via Scholl reaction and Suzuki-Miyaura cross-coupling reactions, illustrated in Scheme 1.[2] All the intermediates and target molecules are confirmed by standard spectroscopic methods. The detailed synthetic procedures are shown in supporting information.

**Synthesis of investigated molecules**

**Compound 1 (1,1,2,2-Tetrakis(4-bromophenyl)ethene)**

Under Ar protection and 0 $^{o}$C, 4,4'-dibromobenzophenone (1.28 g, 4 mmol), Zn powder (0.67 g, 10 mmol) and 45 mL anhydrous THF are added into a 100 mL Schlenk flask. Then, $TiCl_4$ (0.4 g, 2 mmol) is slowly added via syringe. The reaction mixture was stirred for 30 min and akkowed to warm to R.T. and then refluxed for 16 h. After cooling to R.T., the reaction mixture is quenched with $K_2CO_3$ solution and extracted with $CH_2Cl_2$. The obtained organic phase is dried by $Na_2SO_4$, and concentrated by rotary evaporator. The crude solid is purified by column chromatography (DCM : PE = 1 : 1) to obtain a pure compound **1** as a white solid (0.81 g, 62%). 1H NMR (400 MHz, DMSO) δ 7.39 (d, J = 8.5 Hz, 8H), 6.92 (d, J = 8.4 Hz, 8H). HRMS (MALDI-TOF) m/z: [M+] calcd, 647.79; found, 647.78.

**Compound 2**

Under Ar protection, Compound 1 (0.65 g, 1 mmol), 2,3-dichloro-5,6-dicyano-p-benzoquinone (DDQ, 0.45 g, 2 mmol), are involved in a 9 : 1 mixture of $CH_2Cl_2$ and $MeSO_3H$ solution. The reaction mixture is stirred for 24 h under R.T. (around 22-25 $^oC$). Then resulting reaction mixture was quenched by $NaHCO_3$ solution and extracted with CH2Cl2. The obtained organic phase is dried by $Na_2SO_4$, and concentrated by rotary evaporator. The crude solid is purified by column chromatography (DCM : PE = 1 : 1) to obtain a pure compound **2** as a white solid (0.21 g, 32%). 1H NMR (400 MHz, $CDCl_3$) δ 8.75 (d, J = 1.0 Hz, 4H), 8.44 (d, J = 8.0 Hz, 4H), 7.76 (d, J = 10.2 Hz, 4H). HRMS (MALDI-TOF) m/z: [M+] calcd, 643.76; found, 643.76.

**F-TPE**

Compound 2 (0.13 g, 0.2 mmol), 4-methoxy-N-(4-methoxyphenyl)-N-(4-(4,4,5,5-tetramethyl-1,3,2-dioxaborolan-2-yl)phenyl)aniline (0.43 g, 1 mmol), $Pd(PPh_3)_4$ (120 mg, 0.1 mmol), 2 M $K_2CO_3$ (4 mL) in $H_2O$, and DMF (40 mL) are added into a 100 mL flask and then degassed using $N_2$. The mixture was stirring at 95 $^oC$ for 24 h. After cooling to R.T., the reaction mixture is poured into 300 mL cold $Na_2SO_4$ solution, crude product precipitates out as yellow solid. After drying, the solid is purified by column chromatography (DCM : PE = 2: 1) to obtain a pure **F-TPE** as a yellow solid (0.22 g, 71%). $^1H$ NMR (400 MHz, DMSO) δ 1H NMR (400 MHz, DMSO) δ 8.92 (s, 4H), 8.48 (d, J = 8.5 Hz, 4H), 7.87 – 7.64 (m, 12H), 7.05 (d, J = 8.6 Hz, 16H), 6.91 (dd, J = 19.5, 8.5 Hz, 24H), 3.75 (s, 24H). Anal. Calcd. for C106H84N4O8 (%) C, 82.57; H, 5.49; N, 3.63. Found: C, 82.56; H, 5.50; N, 3.62. MS (MALDI-TOF) m/z: [M+] calcd, 1541.63; found 1541.64.

**Device Fabrication and Characterization**

The PSCs in this work were fabricated according to our reports.[3] It should be noted that the concentration of dopant-free HTMs is 20 mg $mL^{-1}$. The concentration of doped HTM is 30 mg $mL^{-1}$ with 15 µL of 4-tert-butylpyridine and 8 µL of lithium bis(trifluoromethylsulphonyl)imide (520 mg $mL^{-1}$ in acetonitrile). The HTM was

deposited on the on FTO/bl-$TiO_2$/mp-$TiO_2$/perovskite substrate by spin-coating at 3000 rpm for 30 s.

Firstly, FTO glass plates were sequentially cleaned by ultrasonic bath, deionized water and ethanol. Using spray pyrolysis methods, the compact $TiO_2$ layer was deposited on clean FTO substrate at 500 °C in which a precursor solution of 0.6 mL titanium diisopropoxide and 0.4 mL bis(acetylacetonate) dissolved in 7 mL isopropanol. Mesoporous $TiO_2$ layer was deposited on above obtained substrate by spin-coating of a diluted particle $TiO_2$ paste (Dyesol 30NR-T, 1:5 w/w diluted in ethanol) at 4500 rpm for 30 s. Subsequently, the substrates were annealed at around 500 °C for 30 min. After cooling down, the perovskite layer was deposited through spin-coating the perovskite precursor solution by a one-step solvent engineering procedure. The perovskite precursor solution includes $PbI_2$ (1.1 M), $PbBr_2$ (0.2 M), MABr (0.2 M), and FAI (1 M), dissolved in a mixed solvent of DMF and DMSO solution (1000 μL, volume ratio 7 : 3). The spin-coating procedure was performed first 1000 rpm for 10 s, second 5000 rpm for 30 s. 100 μL chlorobenzene is dripped on the spinning substrate during the second spin-coating step 15 s at the middle of the procedure. The obtained substrate is immediately heated at 100 °C for 1.5 h on a hotplate. The HTM was subsequently deposited on the substrate by spin-coating at 5000 rpm for 30 s after above substrate cooling to R.T.. The HTM solution were prepared in anhydrous chlorobenzene. the concentration of dopant-free HTMs is 20 mg $mL^{-1}$. The concentration of doped HTM is 30 mg $mL^{-1}$ with 8 μL of 4-tert-butylpyridine and 15 μL of lithium bis(trifluoromethylsulphonyl)imide (520 mg $mL^{-1}$ in acetonitrile). The HTM was deposited on the on FTO/bl-$TiO_2$/mp-$TiO_2$/perovskite substrate by spin-coating at 3000 rpm for 30 s. Finally, a ~70 nm thick Au counter electrode was deposited on top of above film by thermal evaporation. The active area of the device was defined by a black mask with a size of 0.09 $cm^2$ for all measurement.

**Characterization**

The used instrumentations in this work can be found in literature,[3-6] and the detailed experimental methods are also illustrated as follows. $^1H$ NMR spectra were recorded

on a Brücker spectrometer (400 MHz) with chemical shifts against tetramethylsilane (TMS). Time-of-flight mass spectrometer (MALDI-TOF-MS) experiments were recorded using a MS Bruker Daltonik Reflex III and Bruker solariX spectrometer. UV-vis spectra of investigated molecules are carried out on a UV-vis spectrophotometer (SOLID3700, Shimadzu Co. Ltd, Japan). The PL measurements of HTM and perovskite/HTM films were measured on a fluorescence detector (Hitachi F-4600, Japan). Cyclic voltammetry was tested with a CHI660d electrochemical analyzer (CH Instruments, Inc., China). A normal three electrode system was used consisting of a platinum wire counter electrode, a platinum working electrode, as well as a calomel reference electrode. Redox potential of investigated compounds was tested in DCM with 0.1 M tetrabutylammonium hexafluorophosphate with a scan rate of 50 mV $s^{-1}$. Scanning electron microscope (SEM) Fig.s were recorded on a field emission scanning electron microscope (Hitachi SU8010, Japan). The incident photon-to-current conversion efficiency (IPCE) was recorded on QE/IPCE measurement kit (Newport, USA). The moisture resistance of HTMs was measured on a contact angle tester (METATEST E3-300).

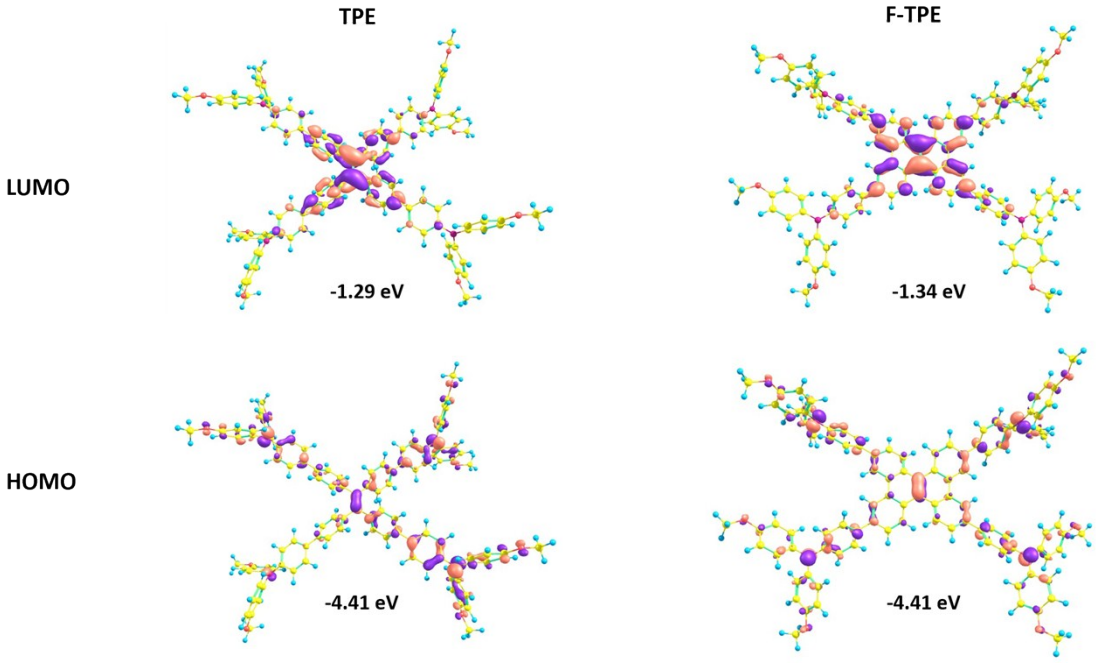


**Fig. S1** Electronic density distributions of the frontier molecular orbitals for **TPE** and **F-**

**TPE**.

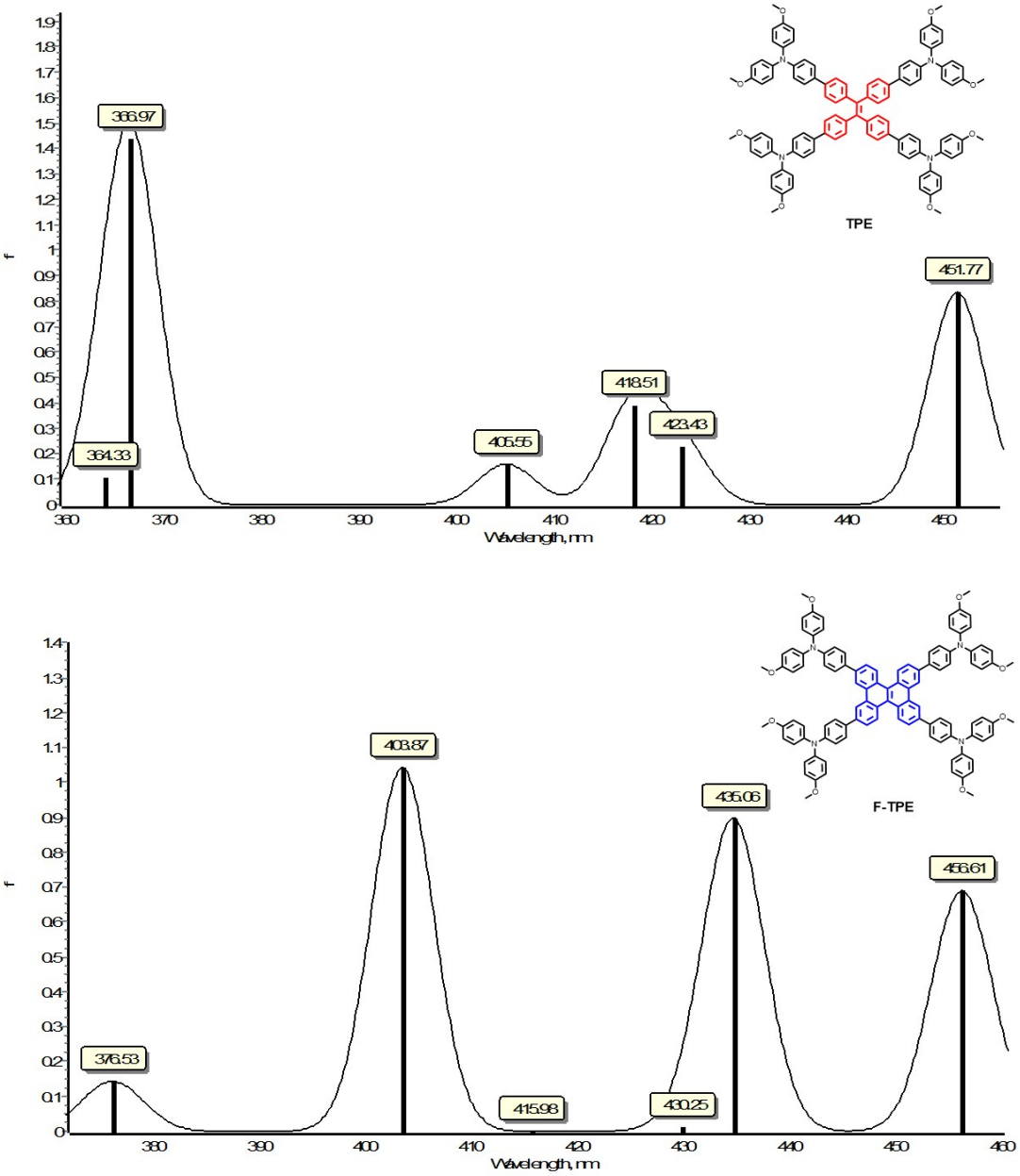


**Fig. S2** Calculated absorption spectra of **TPE** and **F-TPE** at the TDDFT/B3LYP/6-311G* level of theory.

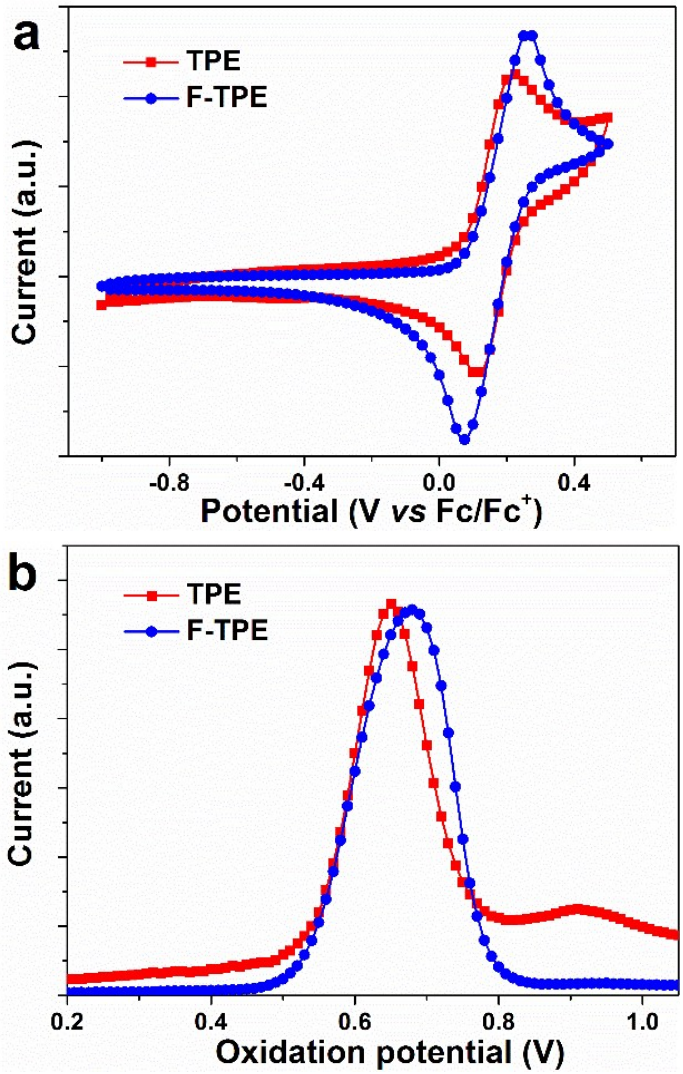


**Fig. S3** (a) Cyclic voltammograms with ferrocene as reference, and (b) differential pulse voltammetry curves of **TPE** and **F-TPE**.

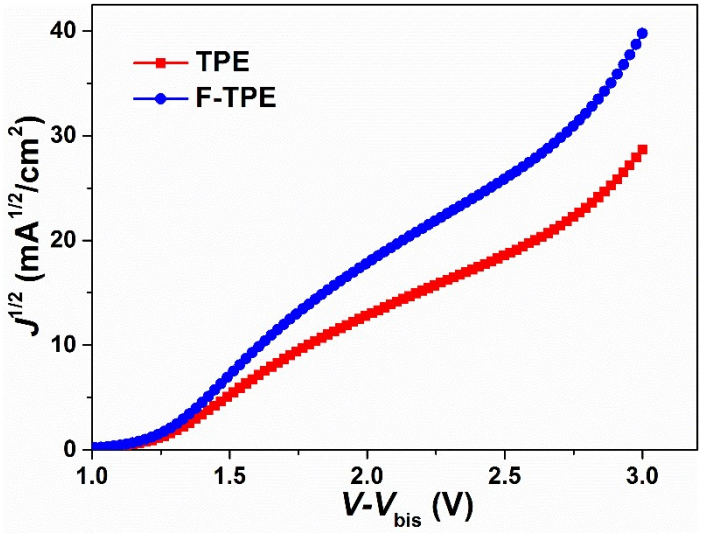


**Fig. S4** Injection characteristics of hole-only devices with a structure of

ITO/PEDOT:PSS/HTM/Au.

The charge carrier mobility of the HTM films were measured using the space-charge-limited current (SCLC) technique. Hole-only devices were fabricated in a structure of ITO/PEDOT:PSS/HTM/Au. The device characteristics were extracted by modeling the dark current under forward bias using the SCLC expression described by the Mott-Gurney law:

$$J = \frac{9}{8}\varepsilon_r \varepsilon_0 \mu \frac{V^2}{L^3}$$

Here, $\varepsilon_r = 3$ is the average dielectric constant of the film, $\varepsilon_0$ is the permittivity of the free space, $\mu$ is the carrier mobility, *L* is the thickness of the film, and *V* is the applied voltage.

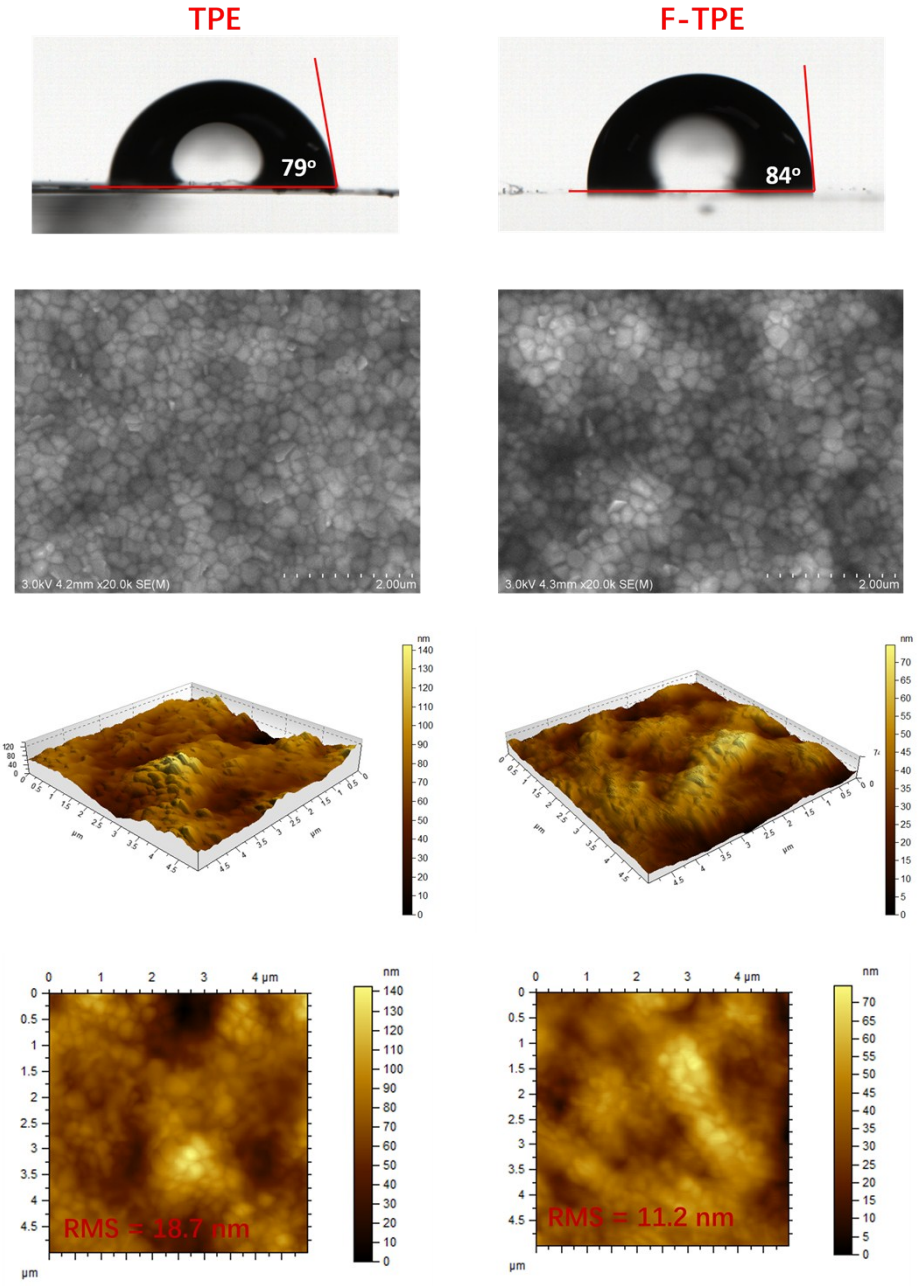


**Fig. S5** Water contact angles of **TPE** and **F-TPE** coated on FTO, SEM and AFM images of the perovskite layers covered by **TPE** and **F-TPE**, respectively.

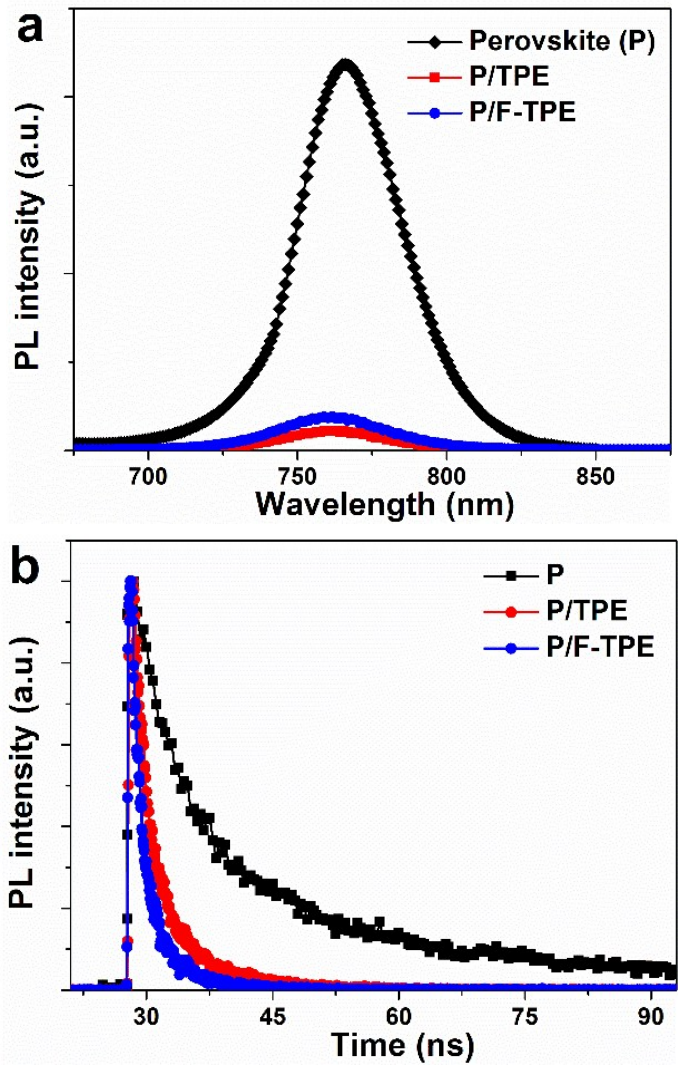


**Fig. S6** (a) TIPL, excitation wavelength: 488 nm, and (b) TRPL of perovskite, perovskite/**TPE** and perovskite/**F-TPE**, excitation wavelength: 488 nm, monitored wavelength: 765 nm.

**Table S1** Detailed device parameters of perovskite solar cells with different dopant-free or doped **TPE** and **F-TPE**.

| HTM | Concentration (mg $mL^{-1}$) | $V_{oc}$ (V) | $J_{sc}$ (mA $cm^{-2}$) | FF (%) | PCE (%) |
|---|---|---|---|---|---|
| dopant-free **TPE** | 10 | 1.03 | 17.32 | 61 | 10.88 |
| dopant-free **TPE** | 10 | 1.02 | 16.98 | 62 | 10.75 |

| | | | | | |
|---|---|---|---|---|---|
| dopant-free **TPE** | 10 | 1.02 | 17.06 | 63 | 10.95 |
| dopant-free **TPE** | 10 | 1.01 | 17.14 | 63 | 10.93 |
| dopant-free **TPE** | 10 | 1.02 | 16.84 | 60 | 10.28 |
| dopant-free **TPE** | 10 | 1.03 | 17.21 | 62 | 10.98 |
| dopant-free **TPE** | 10 | 1.00 | 17.35 | 61 | 10.83 |
| dopant-free **TPE** | 10 | 1.02 | 17.52 | 60 | 10.73 |
| dopant-free **TPE** | 30 | 1.02 | 16.42 | 54 | 9.05 |
| dopant-free **TPE** | 30 | 1.01 | 16.27 | 56 | 9.24 |
| dopant-free **TPE** | 30 | 1.01 | 15.95 | 56 | 9.01 |
| dopant-free **TPE** | 30 | 1.02 | 16.07 | 54 | 8.87 |
| dopant-free **TPE** | 30 | 1.01 | 16.34 | 55 | 9.08 |
| dopant-free **TPE** | 30 | 1.00 | 16.75 | 54 | 9.05 |
| dopant-free **TPE** | 30 | 1.01 | 15.76 | 54 | 8.63 |
| dopant-free **TPE** | 30 | 1.02 | 16.08 | 57 | 9.32 |
| dopant-free **TPE** | 50 | 0.95 | 14.78 | 52 | 7.31 |
| dopant-free **TPE** | 50 | 0.93 | 14.81 | 51 | 7.02 |
| dopant-free **TPE** | 50 | 0.97 | 14.58 | 52 | 7.35 |
| dopant-free **TPE** | 50 | 0.96 | 14.35 | 50 | 6.85 |
| dopant-free **TPE** | 50 | 0.96 | 15.01 | 50 | 7.21 |
| dopant-free **TPE** | 50 | 0.95 | 14.96 | 52 | 7.39 |
| dopant-free **TPE** | 50 | 0.98 | 14.33 | 53 | 7.42 |
| dopant-free **TPE** | 50 | 0.97 | 15.01 | 54 | 7.83 |
| dopant-free **F-TPE** | 10 | 1.06 | 17.98 | 68 | 12.98 |
| dopant-free **F-TPE** | 10 | 1.05 | 18.21 | 69 | 13.11 |
| dopant-free **F-TPE** | 10 | 1.04 | 18.17 | 66 | 12.49 |
| dopant-free **F-TPE** | 10 | 1.05 | 18.53 | 67 | 13.02 |
| dopant-free **F-TPE** | 10 | 1.06 | 18.05 | 65 | 12.45 |
| dopant-free **F-TPE** | 10 | 1.04 | 17.86 | 66 | 12.27 |
| dopant-free **F-TPE** | 10 | 1.04 | 18.09 | 68 | 12.80 |

| | | | | | |
|---|---|---|---|---|---|
| dopant-free **F-TPE** | 10 | 1.05 | 18.44 | 67 | 12.96 |
| dopant-free **F-TPE** | 30 | 1.05 | 17.88 | 64 | 12.04 |
| dopant-free **F-TPE** | 30 | 1.02 | 17.92 | 65 | 11.87 |
| dopant-free **F-TPE** | 30 | 1.03 | 18.03 | 65 | 12.08 |
| dopant-free **F-TPE** | 30 | 1.05 | 17.59 | 63 | 11.64 |
| dopant-free **F-TPE** | 30 | 1.02 | 17.68 | 65 | 11.72 |
| dopant-free **F-TPE** | 30 | 1.02 | 17.66 | 62 | 11.13 |
| dopant-free **F-TPE** | 30 | 1.03 | 17.81 | 64 | 11.74 |
| dopant-free **F-TPE** | 30 | 1.02 | 17.69 | 65 | 11.73 |
| dopant-free **F-TPE** | 50 | 1.03 | 16.81 | 61 | 10.55 |
| dopant-free **F-TPE** | 50 | 1.03 | 17.01 | 58 | 10.13 |
| dopant-free **F-TPE** | 50 | 1.02 | 16.89 | 60 | 10.34 |
| dopant-free **F-TPE** | 50 | 1.02 | 16.78 | 61 | 10.46 |
| dopant-free **F-TPE** | 50 | 1.02 | 16.91 | 59 | 10.14 |
| dopant-free **F-TPE** | 50 | 1.03 | 16.95 | 58 | 10.12 |
| dopant-free **F-TPE** | 50 | 1.02 | 16.83 | 57 | 9.77 |
| dopant-free **F-TPE** | 50 | 1.02 | 16.72 | 58 | 9.86 |
| doped **TPE** | 10 | 1.05 | 20.07 | 68 | 14.33 |
| doped **TPE** | 10 | 1.01 | 19.85 | 65 | 13.00 |
| doped **TPE** | 10 | 1.02 | 18.97 | 67 | 12.97 |
| doped **TPE** | 10 | 1.04 | 20.18 | 64 | 13.42 |
| doped **TPE** | 10 | 1.03 | 19.56 | 63 | 12.71 |
| doped **TPE** | 10 | 1.05 | 19.84 | 64 | 13.32 |
| doped **TPE** | 10 | 1.08 | 20.41 | 66 | 14.51 |
| doped **TPE** | 10 | 1.06 | 20.11 | 68 | 14.48 |
| doped **TPE** | 30 | 1.08 | 20.53 | 71 | 15.75 |
| doped **TPE** | 30 | 1.07 | 20.46 | 70 | 15.33 |
| doped **TPE** | 30 | 1.07 | 20.87 | 71 | 15.84 |
| doped **TPE** | 30 | 1.06 | 19.97 | 72 | 15.25 |

| | | | | | |
|---|---|---|---|---|---|
| doped **TPE** | 30 | 1.06 | 20.48 | 71 | 15.41 |
| doped **TPE** | 30 | 1.07 | 20.63 | 69 | 15.25 |
| doped **TPE** | 30 | 1.08 | 20.06 | 71 | 15.39 |
| doped **TPE** | 30 | 1.07 | 19.95 | 70 | 14.96 |
| doped **TPE** | 50 | 1.07 | 19.95 | 70 | 14.96 |
| doped **TPE** | 50 | 1.06 | 20.61 | 68 | 14.87 |
| doped **TPE** | 50 | 1.05 | 20.34 | 70 | 14.92 |
| doped **TPE** | 50 | 1.07 | 19.87 | 71 | 15.12 |
| doped **TPE** | 50 | 1.08 | 20.19 | 69 | 15.05 |
| doped **TPE** | 50 | 1.06 | 19.62 | 70 | 14.56 |
| doped **TPE** | 50 | 1.05 | 20.28 | 71 | 15.12 |
| doped **TPE** | 50 | 1.06 | 19.48 | 68 | 14.02 |
| doped **F-TPE** | 10 | 1.08 | 19.14 | 70 | 14.45 |
| doped **F-TPE** | 10 | 1.06 | 19.27 | 72 | 14.70 |
| doped **F-TPE** | 10 | 1.10 | 20.17 | 72 | 15.96 |
| doped **F-TPE** | 10 | 1.08 | 19.46 | 71 | 14.94 |
| doped **F-TPE** | 10 | 1.07 | 19.17 | 73 | 14.95 |
| doped **F-TPE** | 10 | 1.08 | 19.52 | 70 | 14.75 |
| doped **F-TPE** | 10 | 1.01 | 19.43 | 71 | 13.94 |
| doped **F-TPE** | 10 | 1.08 | 19.22 | 75 | 15.57 |
| doped **F-TPE** | 30 | 1.09 | 20.88 | 78 | 17.78 |
| doped **F-TPE** | 30 | 1.12 | 21.31 | 76 | 18.16 |
| doped **F-TPE** | 30 | 1.09 | 20.96 | 77 | 17.63 |
| doped **F-TPE** | 30 | 1.11 | 21.52 | 76 | 18.15 |
| doped **F-TPE** | 30 | 1.10 | 20.79 | 77 | 17.63 |
| doped **F-TPE** | 30 | 1.10 | 21.28 | 76 | 17.75 |
| doped **F-TPE** | 30 | 1.09 | 20.94 | 75 | 17.14 |
| doped **F-TPE** | 30 | 1.11 | 21.35 | 77 | 18.30 |
| doped **F-TPE** | 50 | 1.09 | 21.29 | 75 | 17.43 |

| | | | | | |
|---|---|---|---|---|---|
| doped **F-TPE** | 50 | 1.1 | 21.23 | 75 | 17.45 |
| doped **F-TPE** | 50 | 1.09 | 21.04 | 75 | 17.22 |
| doped **F-TPE** | 50 | 1.1 | 20.54 | 74 | 16.70 |
| doped **F-TPE** | 50 | 1.11 | 21.49 | 76 | 18.11 |
| doped **F-TPE** | 50 | 1.08 | 21.28 | 76 | 17.45 |
| doped **F-TPE** | 50 | 1.1 | 21.11 | 76 | 17.65 |
| doped **F-TPE** | 50 | 1.09 | 20.36 | 75 | 16.63 |
| doped spiro-OMeTAD | 73 | 1.08 | 22.10 | 76 | 18.09 |
| doped spiro-OMeTAD | 73 | 1.09 | 22.31 | 75 | 18.16 |
| doped spiro-OMeTAD | 73 | 1.09 | 22.06 | 75 | 18.01 |
| doped spiro-OMeTAD | 73 | 1.09 | 21.81 | 76 | 18.10 |

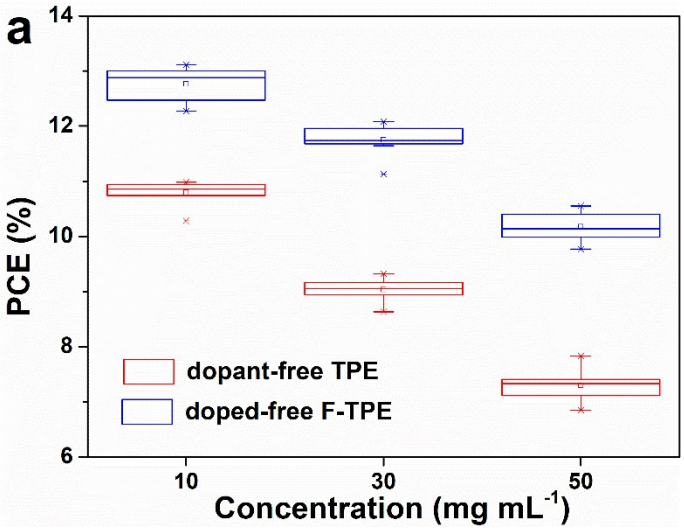

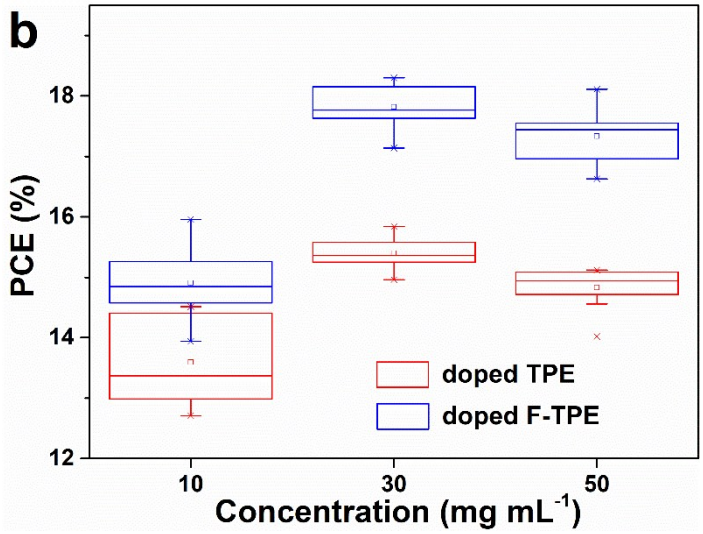


**Fig. S7** The PCE variations along with the concentration change of (a) pristine, and (b) doped HTMs for Table S1.

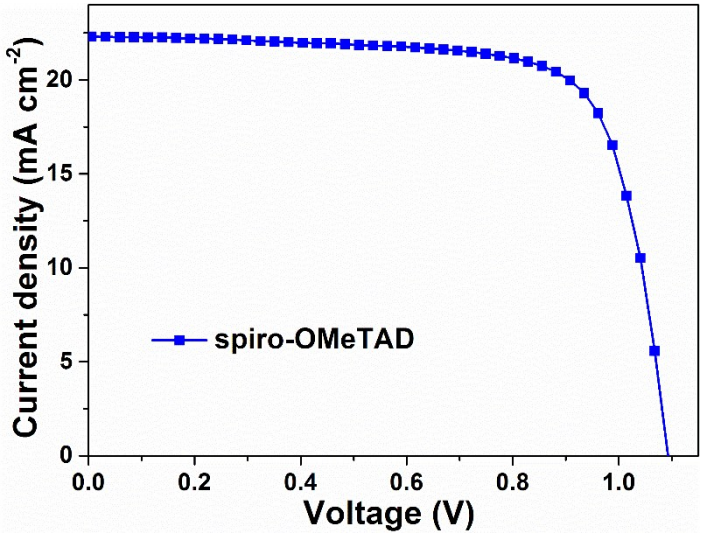


**Fig. S8** *J-V* curves of the best devices employing doped spiro-OMeTAD under the same condition with **TPE** and **F-TPE** in this work.

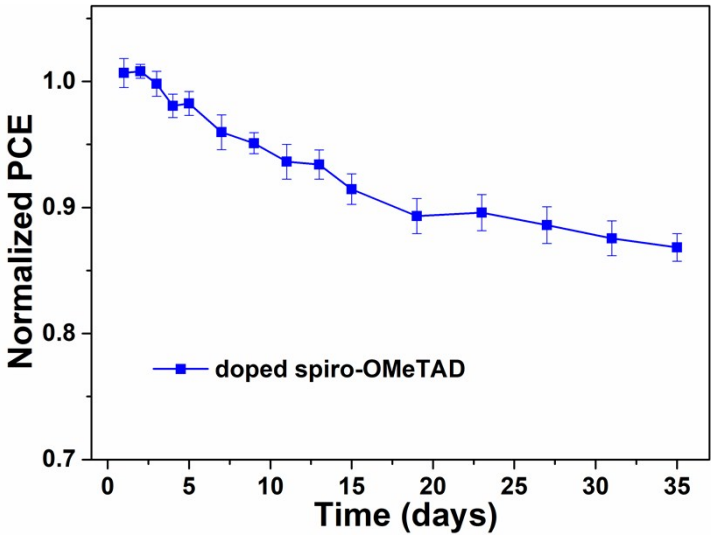


**Fig. S9** stability test for the devices with doped spiro-OMeTAD for reference. Error bars represent standard deviations of 4 individual cells for each case.

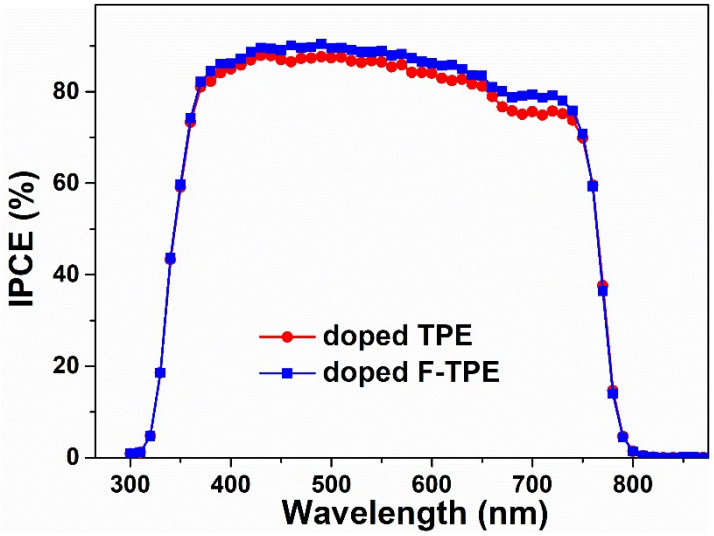


**Fig. S10** IPCE spectra of the devices employing doped **TPE** or **F-TPE**.

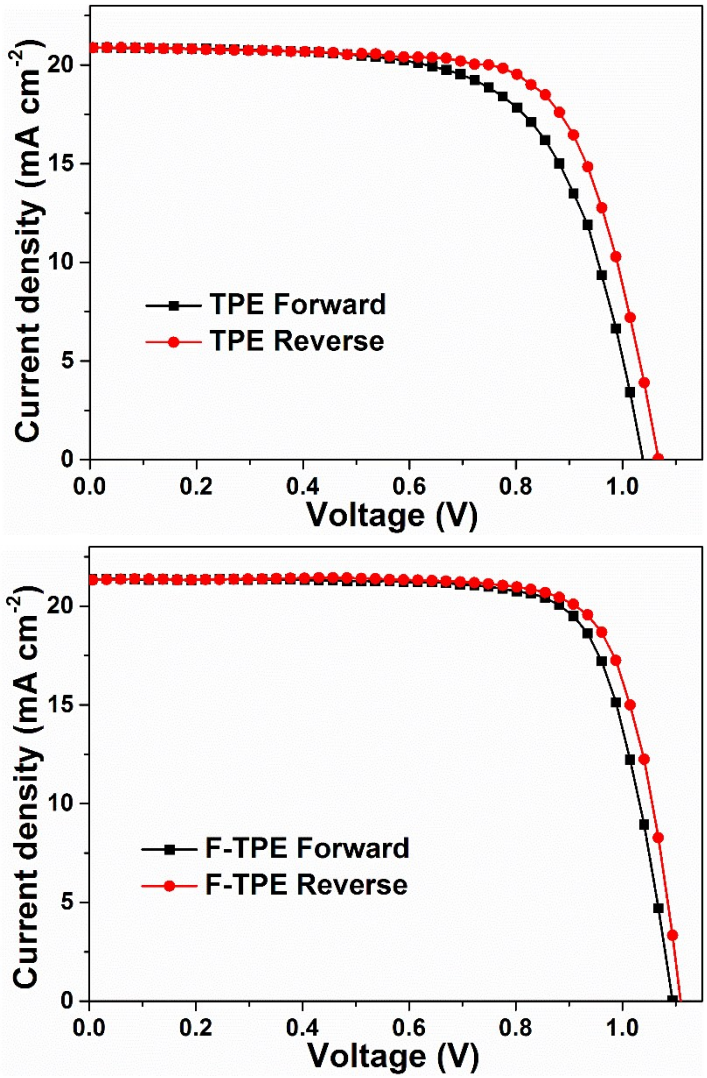


**Fig. S11** *J-V* curves measured by forward scan (from short circuit to open circuit) and reverse scan (from open circuit to short circuit) of the PSCs with different HTMs under AM 1.5 illumination.

**Table S2** Photovoltaic parameters of best-performing PSCs with doped HTMs and measured through forward and reverse scans for Fig. S11.

| | HTM | $V_{oc}$ (V) | $J_{sc}$ (mA cm$^{-2}$) | FF (%) | PCE (%) |
|---|---|---|---|---|---|
| **TPE** | **Forward** | 1.04 | 20.89 | 66 | 14.31 |
| | **Reverse** | 1.07 | 20.87 | 71 | 15.84 |
| **F-TPE** | **Forward** | 1.09 | 21.34 | 76 | 17.73 |
| | **Reverse** | 1.11 | 21.35 | 77 | 18.30 |

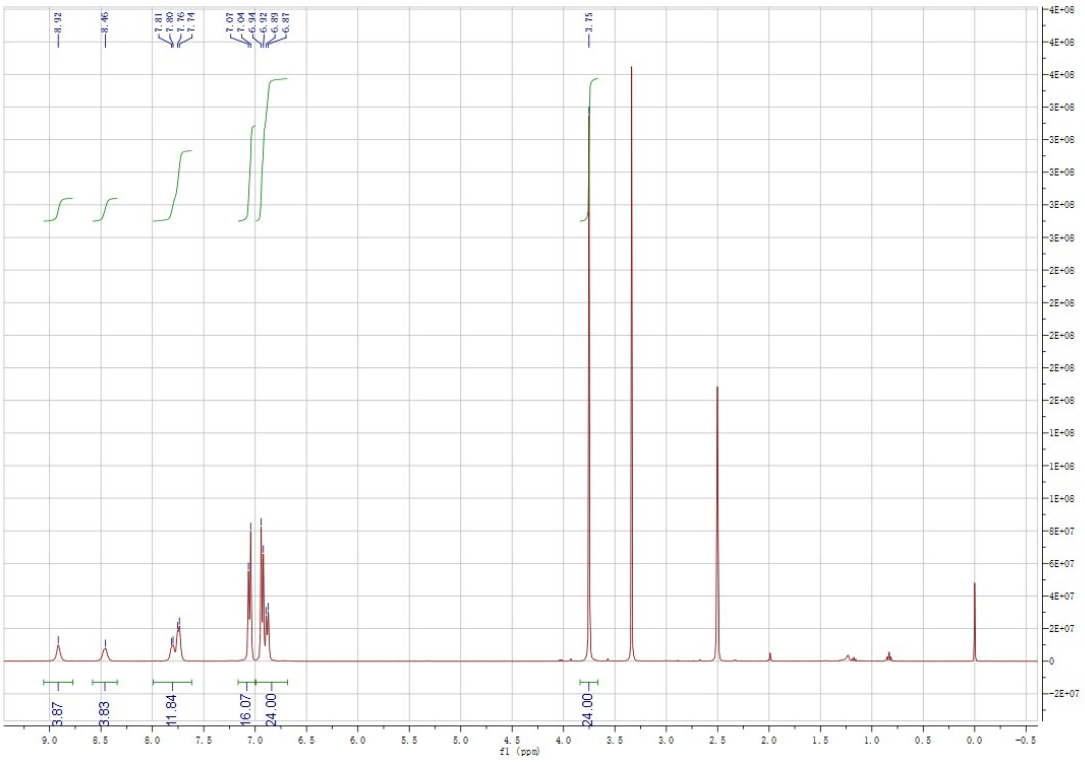


Fig. S12. $^{1}$H-NMR of **F-TPE**.

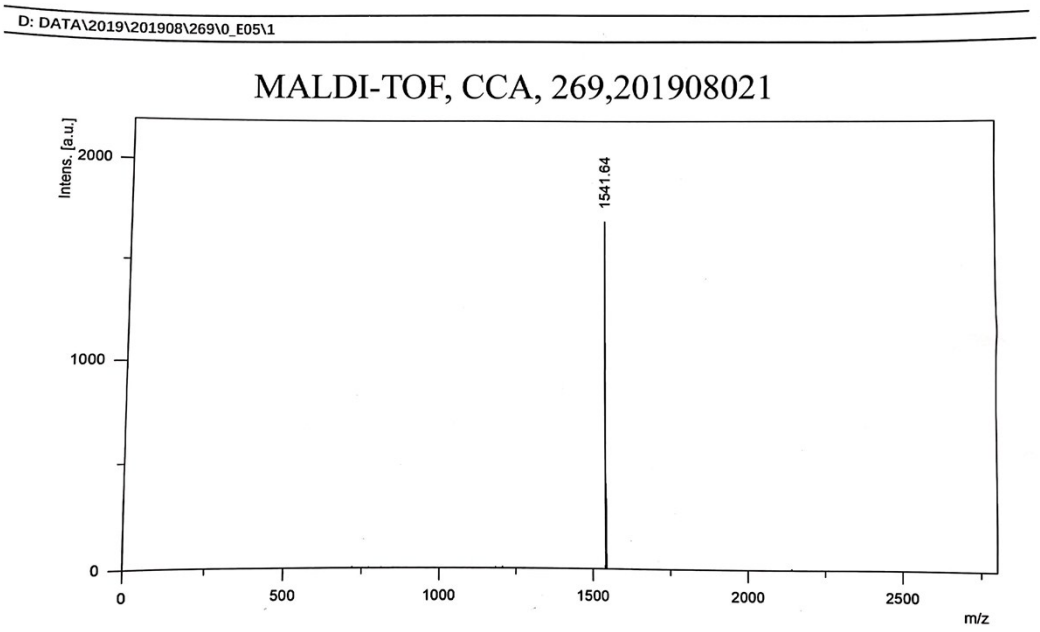


Fig. S13. HRMS (MALDI-TOF) of **F-TPE**.

**A simple analysis of relative costs of spiro-OMeTAD and F-TPE**

The lab synthesis cost of **F-TPE** are estimated on a model originally proposed by Osedach *et al.*[7] Recently, Pertrus and Malinauskas *et al*.[8-10] has used the model to estimate the cost of hole transporting materials. For every synthetic step the required amounts of reactants, catalysts, reagents and solvents are calculated to obtain 1 gram of **F-TPE** are reported (Table S6).

**Table S3** Materials, quantities and cost for the synthesis of **compound 1** (1,1,2,2-Tetrakis(4-bromophenyl)ethene).

| Chemical | Weight Reagent or solvent (g/g) | Price of chemical ($/g) | Cost of chemical ($/g product) | Total cost ($/g) |
|---|---|---|---|---|
| 4,4'-dibromobenzophenone | 1.57 | 1.0 | 1.57 | |
| Zn | 0.82 | 0.04 | 0.03 | |
| THF | 50 | 0.02 | 1 | |
| $TiCl_4$ | 1.5 | 0.02 | 0.03 | |
| $K_2CO_3$ | 2.0 | 0.01 | 0.02 | |
| $Na_2SO_4$ | 2.0 | 0.01 | 0.02 | |
| $CH_2Cl_2$ | 450 | 0.004 | 1.35 | |
| Petroleum ether | 260 | 0.003 | 0.52 | |
| **compound 1** | | | | 4.54 |

**Table S4** Materials, quantities and cost for the synthesis of **compound 2**.

| Chemical | Weight Reagent or solvent (g/g) | Price of chemical ($/g) | Cost of chemical ($/g product) | Total cost ($/g) |
|---|---|---|---|---|
| Compound 1 | 3.25 | 4.54 | 14.75 | |
| DDQ | 2.25 | 0.15 | 0.34 | |
| $MeSO_3H$ | 1.0 | 0.05 | 0.05 | |
| $NaHCO_3$ | 1.0 | 0.01 | 0.01 | |
| $Na_2SO_4$ | 2.0 | 0.01 | 0.02 | |
| $CH_2Cl_2$ | 400 | 0.004 | 1.60 | |
| Petroleum ether | 300 | 0.003 | 0.9 | |
| **compound 2** | | | | 17.67 |

**Table S5** Materials, quantities and cost for the synthesis of **F-TPE**.

| Chemical | Weight | Price of | Cost of | Total cost |
|---|---|---|---|---|

| | Reagent or solvent (g/g) | chemical ($/g) | chemical ($/g product) | ($/g) |
|---|---|---|---|---|
| Compound 2 | 0.59 | 17.67 | 10.42 | |
| 4-methoxy-N-(4-methoxyphenyl)-N-(4-(4,4,5,5-tetramethyl-1,3,2-dioxaborolan-2-yl)phenyl)aniline | 1.95 | 8 | 15.60 | |
| $Pd(PPh_3)_4$ | 0.55 | 13 | 7.15 | |
| $K_2CO_3$ | 3 | 0.02 | 0.06 | |
| DMF | 180 | 0.02 | 3.6 | |
| $Na_2SO_4$ | 4 | 0.01 | 0.04 | |
| $CH_2Cl_2$ | 500 | 0.004 | 2.0 | |
| Petroleum ether | 300 | 0.003 | 0.9 | |
| **F-TPE** | | | | 39.77 |

**Table S6** Survey of the estimated chemical synthesis cost for different HTMs.

| compound | **Material cost ($/g)** | **Commercial price ($/g)** |
|---|---|---|
| **F-TPE** | 39.77 | - |
| Spiro-OMeTAD | 91.67[8-10] | 170-500[8-10] |

## Reference


1. W. Ke, P. Priyanka, S. Vegiraju, C. C. Stoumpos, I. Spanopoulos, C. M. M. Soe, T. J. Marks, M.-C. Chen and M. G. Kanatzidis, J. Am. Chem. Soc., 2017, 140, 388-393.
2. L. Zhai, R. Shukla and R. Rathore, Org. Lett., 2009, 11, 3474-3477.
3. X. Liu, S. Ma, Y. Ding, J. Gao, X. Liu, J. Yao and S. Dai, Solar RRL, 2019, 3, 1800337.
4. X. Liu, X. Ding, Y. Ren, Y. Yang, Y. Ding, X. Liu, A. Alsaedi, T. Hayat, J. Yao and S. Dai, J. Mater. Chem. C, 2018, 6, 12912-12918.
5. M. Li, S. Ma, M. Mateen, X. Liu, Y. Ding, J. Gao, Y. Yang, X. Zhang, Y. Wu and S. Dai, Solar Energy, 2020, 195, 618-625.

6. M. Mateen, Z. Arain, X. Liu, C. Liu, Y. Yang, Y. Ding, S. Ma, Y. Ren, Y. Wu, Y. Tao, P. Shi and S. Dai, J. Power Sources, 2019, 227386.
7. T. P. Osedach, T. L. Andrew and V. Bulović, Energy Environ. Sci., 2013, 6, 711-718.
8. M. L. Petrus, T. Bein, T. J. Dingemans and P. Docampo, J. Mater. Chem. A, 2015, 3, 16874-16874.
9. T. Malinauskas, M. Saliba, T. Matsui, M. Daskeviciene, S. Urnikaite, P. Gratia, R. Send, H. Wonneberger, I. Bruder and M. Grätzel, Energy Environ. Sci., 2016, 9, 1681-1686.
10. M. Saliba, S. Orlandi, T. Matsui, S. Aghazada, M. Cavazzini, J. P. Correabaena, P. Gao, R. Scopelliti, E. Mosconi and K. H. Dahmen, Nat. Energy, 2016, 1, 15017.